frontiers | Frontiers in Physics

TYPE Original Research
PUBLISHED 18 October 2022
DOI 10.3389/fphy.2022.1002512

OPEN ACCESS

EDITED BY
Gaogao Dong,
Jiangsu University, China

REVIEWED BY
Gui-Quan Sun,
North University of China, China
Chengyi Xia,
Tiangong University, China

*CORRESPONDENCE
Hua Li,
lh1@ustl.edu.cn

SPECIALTY SECTION
This article was submitted to Social Physics,
a section of the journal
Frontiers in Physics

RECEIVED 26 July 2022
ACCEPTED 28 September 2022
PUBLISHED 18 October 2022

CITATION
Lv R, Li H, Sun Q and Li B (2022), Stability analysis and optimal control of a time-delayed panic-spreading model.
Front. Phys. 10:1002512.
doi: 10.3389/fphy.2022.1002512

Stability analysis and optimal control of a time-delayed panic-spreading model

Rongjian Lv[1], Hua Li[2]*, Qiubai Sun[2] and Bowen Li[1]

[1]School of Electronics and Information Engineering, University of Science and Technology Liaoning, Anshan, China, [2]School of Business Administration, University of Science and Technology Liaoning, Anshan, China

In emergencies, the transmission of false and uncertain information from individual to individual causes group panic, which in turn leads to the spread of negative emotions in the group. To explore the process of panic spreading in groups, an improved panic-spreading model is constructed in this study. First, the groups are divided into the impatient group and the level-headed group, based on the theory of personality traits in psychology. Second, the logistic model is used to express the growth in the number of susceptible individuals subject to emergencies. Third, the delay effect of panic in the group can have an influence on the spread of panic. Therefore, a time-delayed panic-spreading model considering the epidemic model is established. The threshold value of the model is calculated, and the conditions for the local and global stability of the panic-free equilibrium and panic-permanent equilibrium are obtained by analyzing the dynamic behavior of the delayed-time panic model. On this basis, we choose the intensity of government measures as control variables and establish an optimal control model to minimize the spread scale. The existence and necessary conditions of the optimal solution are proved. Finally, the correctness of the conclusion is verified by numerical simulations.

KEYWORDS

panic spreading, time-delay, stability analysis, optimal control, numerical simulation

1 Introduction

With the rapid development and progress of the global economy, the security of emergencies has become a very hot topic in daily life. High-rise buildings and intensive places are increasing, and these places attract a large number of people, triggering social stability and public safety in the case of fires, earthquakes, and a series of other emergencies. Such emergencies can generate negative emotions, such as agitation, and panic can spread through the group [1–4], thus generating a herding behavior and leading to group clogging [5]. Therefore, it is important to model emotions during emergencies.

Epidemic models are widely used in the construction of transmission models due to their own characteristics, such as rumor spread [6–8], virus spread [9, 10], and emotion spread [11, 12]. For example, Hu et al. [13] established a rumor model considering the proportion of wise men in a crowd and studied its effect on rumor spread. Jiang et al. [14] proposed a new rumor model to analyze the interaction mechanism between rumor spreading and debunking processes. Liu et al. [15] constructed a bird-to-human spread model with logistic growth and the Allee effect and explored the dynamic behavior of the model. Chen [16] developed a dynamic model by analyzing the impact of investor sentiment on the stock market and simulated the relevant theoretical results. Zhao et al. [17] applied the SIR model and bond percolation theory to study the multiple route-transmitted epidemic process on multiplex networks, and we obtained the epidemic threshold and outbreak size by calculation. To analyze the impact of patch distribution on virus propagation, Zhao [18] proposed a hybrid patch distribution strategy by combining the advantages of both the traditional-centralized patch distribution strategy and the traditional-decentralized patch distribution strategy. Guo et al. [19] developed a new epidemic model with local mapping relationships in a two-layered time-varying network to study the effect of information diffusion on the spread of epidemics.

However, in natural and social phenomena, the trends of many models are related not only to the current situation but also to past development dynamics, for example, the incubation period of viruses and the delay of transmission signals. Thus, the introduction of a time delay to study the effects caused by such phenomena is widely used in computer networks [20–23] and biological systems [24–26] in many fields. Zheng et al. [27] proposed a two-strain delay model and calculated the threshold and equilibrium point of the model. Wu [28] developed a nonlinear incidence and distributed latent delay model-based SIR and analyzed the traveling waves at the equilibrium point of this model. With COVID-19 as the background, Khan et al. [29] developed a model with random perturbations as well as time delays and obtained the condition for the extinction of the virus. Similarly, Rihan [30] proposed a SIAQR delay model and focused on the spread of the virus in populations. Xia et al. [31] studied the effects of a delayed recovery and nonuniform spread on disease transmission in structured populations. Chen et al. [32] built an improved rumor-spreading model based on considering the delay of an interactive system. By proposing the correlated strategies, this study could control rumor spreading. Zhang et al. [33] found a time-delay model when public opinions transformed and analyzed the effect of time delay on the equilibrium point. Hu [34] modeled the spread of reaction–diffusion rumors with time delay as well as their variations based on complex networks and studied the diffusion around the equilibrium point of the model and the Turing bifurcation.

Emergencies lead to the spread of uncertain information and panic, and the government should take effective measures, such as releasing official information and suppressing by force. The application of such measures can be referred to as the optimal control problem. The aim is to use the minimum cost while controlling emergencies. Bolzoni et al. [35] considered the time–optimal control problem in an epidemic model, and an analysis of the optimal strategy could reduce viral transmission. Grandits [36] investigated a stochastic control epidemic model and used the HJB equation to explore optimal control strategies. Dai [37] considered the semigroup theory and minimizing sequences to prove existence and some estimates of the unique strong solution and optimal pair of optimal control problems, respectively. Hang et al. [38] proposed an optimal control avian influenza model with delay and analyzed the results using Pontryagin's maximum principle. Bashier [39] developed an optimal control model by delay differential equations based on the SIR epidemic model and studied the sensitivity of the two strategies to time delays. Wu [40] investigated nonlinear optimal control problems with multiple time delays using gradient-based optimization algorithms. To address the dynamics virus spread model, Sun et al. [41] formulated a model of disseminated FMD with a fixed incubation period and non-localized infection to explore effective control measures. Kouidere et al. [42] proposed an optimal control approach with delays in state and control variables. Measures have been proposed in the literature on how to control the current spread of COVID-19. Among them, wearing masks and vaccination are effective measures. Based on the implementation of the New York City policy, Ma et al. [43] established a dynamic model incorporating effective mask coverage to assess the impact of mask use during the COVID-19 epidemic. Ruhomally et al. [44] developed a cellular automaton (CA) describing the dynamics of COVID-19 and studied the effect of contact tracing and vaccination on the number of two reproductive species. Economy and cost were considered in the prevention and control of COVID-19. Asamoah et al. [45] developed a non-autonomous nonlinear deterministic model to study the control of COVID-19 in order to analyze the cost and economic health outcomes of the autonomous nonlinear model proposed in the Kingdom of Saudi Arabia. The epidemic cannot dissipate due to the mutation of the COVID-19 virus. To predict the future evolution of COVID-19, Massard et al. [46] constructed a model to investigate the impact of three different SARS-CoV-2 variants on the spread of COVID-19 in France from January to May 2021 (before vaccination was extended to the entire population).

The models of time-delay rumors and time-delay viruses and the corresponding optimal control models were reviewed in the aforementioned paragraphs, but the time-delayed panic-spreading model in emergencies was not mentioned. In real life, emotions have an impact on the behavior of individuals, especially panic. At the same time, emotions have three characteristics: process, holistic, and individual variability, among which individual variability is the most significant characteristic. Individual differences in emotions are mainly determined by the personality of an individual. Individuals have different emotion perception abilities. Normally, impatient individuals are emotionally infected and irrational, while level-headed individuals are sensible. Therefore, it is necessary to take into account the difference of different individual personalities in the spread of panic under emergencies, which can truly simulate the process of emotion spread in real life. Therefore, it is of great theoretical and practical importance to explore the effect of time delay on the spread of panic.

The rest of this study is structured as follows: In Section 2, a time-delayed panic-spreading model is presented. In Section 3, the local stability and global stability of two equilibria are studied by mathematical analysis. We develop the corresponding optimal control model and solve necessary conditions for the existence of optimal solutions by the maximum principle of Pontryagin in Section 4. The theoretical results of the numerical simulation analysis are given in Section 5. A brief conclusion is given in Section 6.

2 Model formulation

Individuals in the group realize that the occurrence of emergencies and the panic caused by them have a delayed effect. The delayed model is more in line with the phenomenon after the occurrence of emergencies. Therefore, we establish a time-delayed panic-spreading model considering the epidemic model.

(I) In emergencies, individual differences in characteristics (gender, age, and personality, etc.) can have an effect on individual panic spreading. We mainly consider the effect of individual personality on panic spreading. Therefore, according to personality of the literature [47], the group was divided into the impatient group and the level-headed group. The former is reckless and adventurous and easily influenced by the emotions of others. On the contrary, the latter is wise and thoughtful and will calm down in the face of difficulties. An important aspect of the level-headed group is that panic can spread from the impatient group. However, the impatient group infects within the group. The infection rate of both groups adopts a bilinear infection rate:

$$g(I)S = \beta IS. \tag{1}$$

(II) The number of susceptible individuals increases rapidly due to incomplete knowledge of the occurrence of emergencies. Since the logistic model can considerably take into account the factors that the growth of the number is limited by the environment (e.g., emergency), the logistic growth model is more suitable for the actual situation. Therefore, in the impatient group and the level-headed group, the susceptible individuals follow the classical logistic single-species growth model [48]:

$$\frac{dS}{dt} = rS\left(1 - \frac{S}{K}\right), \tag{2}$$

where K is the carrying capacity and r is the intrinsic increase rate constant.

(III) In emergencies, due to the time required for susceptible individuals to come into contact with the surrounding panicked individuals to become infected individuals, we denote the certain time as the spread delay, which are defined by τ_1 and τ_2.The rate of change of the infected impatient group depends not only on their number at the previous moment $t - \tau_1$ but also on the probability that the infected impatient group survived from the moment $t - \tau_1$ to the moment t. Similarly, the rate of change of the infected level-headed group depends not only on their number at the previous moment $t - \tau_2$ but also on the probability that the infected level-headed group survived from the moment $t - \tau_2$ to the moment t.

(IV) The recovered individuals of the impatient group and the level-headed group experience permanent immunity with probability.

The model can be described as

$$\begin{aligned}
\frac{dS_1}{dt} &= r_1 S_1\left(1 - \frac{S_1}{K_1}\right) - \beta_1 I_1 S_1 - dS_1,\\
\frac{dI_1}{dt} &= e^{-d\tau_1}\beta_1 S_1(t-\tau_1) I_1(t-\tau_1) - (d+\delta_1) I_1,\\
\frac{dR_1}{dt} &= \delta_1 I_1 - dR_1,\\
\frac{dS_2}{dt} &= r_2 S_2\left(1 - \frac{S_2}{K_2}\right) - \beta_2 I_1 S_2 - dS_2,\\
\frac{dI_2}{dt} &= e^{-d\tau_2}\beta_2 S_2(t-\tau_2) I_1(t-\tau_2) - (d+\delta_2) I_2,\\
\frac{dR_2}{dt} &= \delta_2 I_2 - dR_2.
\end{aligned} \tag{3}$$

In this model, both the impatient group and the level-headed group could be divided into three states: susceptible, infected, and recovered, represented as S_1, I_1, and R_1 and S_2, I_2, and R_2 at time t, respectively. d represents the death rate of the individual. β_1 and β_2 are the infection rates of the susceptible impatient group and level-headed group, respectively. δ_1 and δ_2 are the recovery rates of the susceptible impatient group and level-headed group, respectively. τ_1 and τ_2 are the time delays of the susceptible impatient group and level-headed group, respectively.

We assume that the initial conditions are

$$\begin{cases}
S_1(\theta) = \vartheta_1(\theta), I_1(\theta) = \vartheta_2(\theta), R_1(\theta) = \vartheta_3(\theta),\\
S_2(\theta) = \vartheta_4(\theta), I_2(\theta) = \vartheta_5(\theta), R_2(\theta) = \vartheta_6(\theta),\\
\vartheta_i(\theta) \geq 0, \vartheta_i(0) > 0, \quad \theta \in [-\tau, 0] \quad, (\vartheta_i \in C)[-\tau, 0], R_+^6) \quad, \quad i = 1,2,3,4,5,6.
\end{cases} \tag{4}$$

For Model (3), the basic reproduction number can be computed as follows [49, 50]:

$$R_0 = \frac{e^{-d\tau_1}\beta_1 K_1 (r_1 - d)}{r_1 (d + \delta_1)}.$$

3 Stability analysis

It is to be noted that the two recovered equations are independent in Model (3) and have no effect on the dynamic analysis, so Model (3) can be decoupled to obtain the following model:

$$\begin{aligned}\frac{dS_1}{dt} &= r_1 S_1\left(1-\frac{S_1}{K_1}\right)-\beta_1 I_1 S_1 - dS_1,\\ \frac{dI_1}{dt} &= e^{-d\tau_1}\beta_1 S_1(t-\tau_1)I_1(t-\tau_1)-(d+\delta_1)I_1,\\ \frac{dS_2}{dt} &= r_2 S_2\left(1-\frac{S_2}{K_2}\right)-\beta_2 I_1 S_2 - dS_2,\\ \frac{dI_2}{dt} &= e^{-d\tau_2}\beta_2 S_2(t-\tau_2)I_1(t-\tau_2)-(d+\delta_2)I_2.\end{aligned} \tag{5}$$

We discuss the design of Model (5) as follows:

(i) For any feasible parameter, the $E^0 = (0,0,0,0)$ equilibrium point always exists.
(ii) The model has three equilibrium points, namely, $E_1^0 = (\frac{K_1(r_1-d)}{r_1}, 0, \frac{K_2(r_2-d)}{r_2}, 0), E_2^0 = (\frac{K_1(r_1-d)}{r_1}, 0, 0, 0)$, and $E_3^0 = (0, 0, \frac{K_2(r_2-d)}{r_2}, 0)$, provided that the conditions $r_1 - d > 0$ and $r_2 - d > 0$ are met.
(iii) The unique positive equilibrium point $E^* = (S_1^*, I_1^*, S_2^*, I_2^*)$, when $R_0 > 1$, $r_1 - d > 0$, and $r_2 - d - \beta_2 I_1 > 0$. Here, $S_1^* = \frac{d+\delta_1}{\beta_1 e^{-d\tau_1}}$, $I_1^* = \frac{r_1-d}{\beta_1}(1-\frac{1}{R_0})$, $S_2^* = \frac{(d+\delta_2)I_2^*}{\beta_2 e^{-d\tau_2} I_1^*}$, and $I_2^* = (r_2 - d - \beta_2 I_1^*)\frac{K_2\beta_2 I_1^* e^{-d\tau_2}}{r_2(d+\delta_2)}$.

3.1 Stability of panic-free equilibrium

Theorem 3.1. the panic-free equilibrium E_1^0 is locally asymptotically stable if $R_0 < 1$.

Proof. The corresponding characteristic equation of Model (5) at E_1^0 is

$$\left[\lambda-\left(r_1-d-\frac{2r_1S_1}{K_1}\right)\right]\left[\lambda-e^{-(d+\lambda)\tau_1}\beta_1 S_1+(d+\delta_1)\right]\left[\lambda-\left(r_2-d-\frac{2r_2S_2}{K_2}\right)\right][\lambda+(d+\delta_2)]=0. \tag{6}$$

Clearly, according to (6), we obtain the eigenvalues

$$\lambda_1 = -(d+\delta_2) < 0, \tag{7}$$

$$\lambda_2 = r_1 - d - \frac{2r_1S_1}{K_1} = r_1 - d - \frac{2r_1}{K_1}\cdot\frac{K_1(r_1-d)}{r_1} = -(r_1-d) < 0, \tag{8}$$

$$\lambda_3 = r_2 - d - \frac{2r_2S_2}{K_2} = r_2 - d - \frac{2r_2}{K_2}\cdot\frac{K_2(r_2-d)}{r_2} = -(r_2-d) < 0. \tag{9}$$

Then, the other eigenvalue of (6) can be rewritten as

$$f_1(\lambda_4) = e^{-(d+\lambda_4)\tau_1}\beta_1 S_1 - (d+\delta_1) - \lambda_4. \tag{10}$$

If $\tau_1 = 0$ and $R_0 < 1$, then $\lambda_4 = \frac{\beta_1 K_1(r_1-d)}{r_1} - (d+r_1) < 0$. Hence, E_1^0 is locally asymptotically stable.

If $\tau_1 > 0$, assume that $\lambda_4 = i\nu\,(\nu > 0)$ and substitute $i\nu$ into (10). Separating real and imaginary parts by the Euler formula, we can obtain

$$\begin{cases}\dfrac{\beta_1 K_1(r_1-d)e^{-d\tau_1}}{r_1}\cdot\cos(\nu\tau_1) = d+\delta_1,\\ -\dfrac{\beta_1 K_1(r_1-d)e^{-d\tau_1}}{r_1}\cdot i\sin(\nu\tau_1) = i\nu.\end{cases} \tag{11}$$

We square and add the two equations of (11), yielding

$$\nu^2 = \left[\frac{\beta_1 K_1(r_1-d)e^{-d\tau_1}}{r_1}\right]^2 - (d+\delta_1)^2. \tag{12}$$

Since $R_0 < 1$, we can obtain $[\frac{\beta_1 K_1(r_1-d)e^{-d\tau_1}}{r_1}]^2 < (d+\delta_1)^2$. Thus, $\nu^2 < 0$, which is a contradiction, so the roots have a negative real part.

Therefore, if $R_0 < 1$, the panic-free equilibrium E_1^0 is locally asymptotically stable for all $\tau_1 > 0$.

The eigenvalues of equilibrium point E_2^0 are $\lambda_1 = -(r_1-d)$, $\lambda_2 = r_2 - d > 0$, $\lambda_3 = d + \delta_2 > 0$, and $\lambda_4 = \frac{K_1(r_1-d)e^{-(d+\lambda)\tau_1}\beta_1}{r_1} - (d+\delta_1)$, so E_2^0 is not locally asymptotically stable. Similarly, E_3^0 is not locally asymptotically stable.

In summary, the panic-free equilibrium E_1^0 is locally asymptotically stable for $R_0 < 1$.

Theorem 3.2. the panic-free equilibrium E_1^0 is globally asymptotically stable if $R_0 < 1$.

Proof. We study the impatient group submodel as follows:

$$\begin{aligned}\frac{dS_1}{dt} &= r_1 S_1\left(1-\frac{S_1}{K_1}\right)-\beta_1 I_1 S_1 - dS_1,\\ \frac{dI_1}{dt} &= e^{-d\tau_1}\beta_1 S_1(t-\tau_1)I_1(t-\tau_1)-(d+\delta_1)I_1.\end{aligned} \tag{13}$$

The panic-free equilibrium of Submodel (13) is $E_{11}^0 = (S_1^0, I_1^0) = (\frac{K_1(r_1-d)}{r_1}, 0)$.

Therefore, we choose the Lyapunov function as shown in the following equation:

$$V_1 = \left(S_1 - S_1^0 - S_1^0\ln\frac{S_1}{S_1^0}\right) + I_1 + \int_{t-\tau_1}^{t} e^{-d\tau_1}\beta_1 S_1(s)I_1(s)ds. \tag{14}$$

Then,

$$\begin{aligned}\frac{dV_1}{dt} &= \frac{S_1-S_1^0}{S_1}\left[r_1S_1\left(1-\frac{S_1}{K_1}\right)-\beta_1 I_1 S_1 - dS_1\right]\\ &\quad+\left[e^{-d\tau_1}\beta_1 S_1(t-\tau_1)I_1(t-\tau_1)-(d+\delta_1)I_1\right]\\ &\quad+\left[e^{-d\tau_1}\beta_1 S_1^0 I_1 - e^{-d\tau_1}\beta_1 S_1(t-\tau_1)I_1(t-\tau_1)\right]\\ &= -\frac{r_1}{K_1}(S_1-S_1^0)^2 - \beta_1 I_1(S_1-S_1^0) - (d+\delta_1)I_1 + e^{-d\tau_1}\beta_1 S_1^0 I_1\end{aligned} \tag{15}$$

$$= -\frac{r_1}{K_1}(S_1 - S_1^0)^2 - \beta_1 I_1 (S_1 - S_1^0) + (d+\delta_1) I_1 \left[\frac{\beta_1 S_1^0 e^{-d\tau_1}}{(d+\delta_1)} - 1\right]$$
$$= -\frac{r_1}{K_1}(S_1 - S_1^0)^2 - \beta_1 I_1 (S_1 - S_1^0) + (d+\delta_1) I_1 [R_0 - 1] < 0.$$

Since $R_0 < 1$, $\frac{dV_1}{dt} < 0$. Combined with the LaSalle invariance principle, for Submodel (13), the panic-free equilibrium E_{11}^0 is globally asymptotically stable.

Thus, we consider the level-headed group submodel at the none-infected state.

$$\begin{aligned} \frac{dS_2}{dt} &= r_2 S_2\left(1 - \frac{S_2}{K_2}\right) - dS_2,\\ \frac{dI_2}{dt} &= -(d+\delta_2) I_2. \end{aligned} \tag{16}$$

By calculation, we can obtain

$$\begin{aligned} S_2 &= \frac{K_2(r_2 - d)}{r_2} + Ce^{-\frac{r_2}{K_2}t},\\ I_2 &= Ce^{-(d+\delta_2)}t. \end{aligned} \tag{17}$$

Since C is a positive constant, when $t \to \infty$, $S_2 \to \frac{K_2(r_2-d)}{r_2}$, $I_2 \to 0$. Hence, we summarize this result in the following theorem.

If $R_0 < 1$, the panic-free equilibrium E_1^0 is globally asymptotically stable.

3.2 Stability of panic-permanent equilibrium

Theorem 3.3. the panic-permanent equilibrium E^* is locally asymptotically stable if $R_0 > 1$.

Proof. The Jacobian matrix of Model (5) at the panic-permanent equilibrium E^* is

$$J(E^*) = \begin{bmatrix} r_1 - \frac{2r_1 S_1^*}{K_1} - \beta_1 I_1^* - d & -\beta_1 S_1^* & 0 & 0 \\ \beta_1 I_1^* e^{-(d+\lambda)\tau_1} & \beta_1 S_1^* e^{-(d+\lambda)\tau_1} - (d+\delta_1) & 0 & 0 \\ 0 & -\beta_2 S_2^* & r_2 - \frac{2r_2 S_2^*}{K_2} - \beta_2 I_1^* - d & 0 \\ 0 & \beta_2 S_2^* e^{-(d+\lambda)\tau_2} & \beta_2 I_1^* e^{-(d+\lambda)\tau_2} & -(d+\delta_2) \end{bmatrix}. \tag{18}$$

The characteristic equation of the Jacobian matrix (18) is

$$\left\{\left[\lambda - \left(r_1 - d - \beta_1 I_1^* - \frac{2r_1 S_1^*}{K_1}\right)\right]\left[\lambda - e^{-(d+\lambda)\tau_1}\beta_1 S_1^* + (d+\delta_1)\right] + \beta_1 I_1^* e^{-(d+\lambda)\tau_1} \cdot \beta_1 S_1^*\right\}$$
$$\left[\lambda - \left(r_2 - d - \beta_2 I_1^* - \frac{2r_2 S_2^*}{K_2}\right)\right][\lambda + (d+\delta_2)] = 0. \tag{19}$$

We can obtain the eigenvalues by calculating the following equation:

$$\lambda_1 = -(d+\delta_2) < 0.$$
$$\lambda_2 = r_2 - d - \beta_2 I_1^* - \frac{2r_2 S_2^*}{K_2} = r_2\left(1 - \frac{2r_2 S_2^*}{K_2}\right) - d - \beta_2 I_1^*$$
$$= d + \beta_2 I_1^* - \frac{r_2 S_2^*}{K_2} - d - \beta_2 I_1^* = -\frac{r_2 S_2^*}{K_2} < 0.$$

The other two eigenvalues of (19) are rewritten by the following equation:

$$\left[\lambda - \left(r_1 - d - \beta_1 I_1^* - \frac{2r_1 S_1^*}{K_1}\right)\right]\left[\lambda - e^{-(d+\lambda)\tau_1}\beta_1 S_1^* + (d+\delta_1)\right] + \beta_1 I_1^* e^{-(d+\lambda)\tau_1} \cdot \beta_1 S_1^* = 0. \tag{20}$$

Eq. 20 is equivalent to

$$\lambda^2 + M\lambda + N = 0, \tag{21}$$

where

$$M = \left(\beta_1 I_1^* + d + \frac{2r_1 S_1^*}{K_1} - r_1\right) + e^{-(d+\lambda)\tau_1}\beta_1 S_1^* - (d+\delta_1), \tag{22}$$

$$N = \left(r_1 - d - \beta_1 I_1^* - \frac{2r_1 S_1^*}{K_1}\right) \cdot \left[(d+\delta_1) - e^{-(d+\lambda)\tau_1}\beta_1 S_1^*\right] + \beta_1^2 S_1^* I_1^* e^{-(d+\lambda)\tau_1}. \tag{23}$$

If $R_0 > 1$, we easily obtain $d + \delta_1 < e^{-(d+\lambda)\tau_1}\beta_1 S_1$. Since $S_1^* > 0, I_1^* > 0$, and $e^{-(d+\lambda)\tau_1} > 0$, $M > 0$ and $N > 0$. According to Vieta's theorem, Eq. 21 has negative roots.

In summary, the panic-permanent equilibrium E^* is locally asymptotically stable if $R_0 > 1$.

Theorem 3.4. the panic-permanent equilibrium E^* is globally asymptotically stable if $R_0 > 1$.

Proof. We consider the impatient group submodel in the following form:

$$\begin{aligned} \frac{dS_1}{dt} &= r_1 S_1\left(1 - \frac{S_1}{K_1}\right) - \beta_1 I_1 S_1 - dS_1,\\ \frac{dI_1}{dt} &= e^{-d\tau_1}\beta_1 S_1(t-\tau_1) I_1(t-\tau_1) - (d+\delta_1) I_1, \end{aligned} \tag{24}$$

We structure the Lyapunov function as

$$V_2 = V_3 + \frac{e^{d\tau_1}}{\beta_1 S_1^*} V_4 + V_5, \tag{25}$$

$$V_3 = \frac{S_1}{S_1^*} + 1 - \ln\frac{S_1}{S_1^*}, V_4 = \frac{I_1}{I_1^*} + 1 - \ln\frac{I_1}{I_1^*}, \tag{26}$$

$$V_5 = \int_0^{\tau_1}\left(\frac{I_1(t-s)}{I_1^*} + 1 - \ln\frac{S_1(t-s) I_1(t-s)}{S_1^* I_1^*}\right) ds. \tag{27}$$

Since $r_1 = \frac{r_1 S_1^*}{K_1} + \beta_1 I_1^* + d$,

$$\begin{aligned}\frac{dV_3}{dt} &= \frac{1}{S_1^*}\left(1-\frac{S_1}{S_1^*}\right)\left[r_1 S_1\left(1-\frac{S_1}{K_1}\right)-\beta_1 I_1 S_1 - dS_1\right] \\ &= (S_1 - S_1^*)\left[r_1 - \frac{r_1 S_1}{K_1} - \beta_1 I_1 - d\right] \\ &= (S_1 - S_1^*)\left[\frac{r_1 S_1^*}{K_1} + \beta_1 I_1^* + d - \frac{r_1 S_1}{K_1} - \beta_1 I_1 - d\right] \\ &= -\frac{r_1}{K_1}(S_1 - S_1^*)^2 - \beta_1 (S_1 - S_1^*)(I_1 - I_1^*),\end{aligned} \tag{28}$$

when S_1, S_1^* and I_1, I_1^* have the same sign, $(S_1 - S_1^*)(I_1 - I_1^*) > 0$, and $\frac{dV_3}{dt} < 0$.

$$\begin{aligned}\frac{dV_4}{dt} &= \frac{1}{I_1^*}\left(1-\frac{I_1}{I_1^*}\right)\left[e^{-d\tau_1}\beta_1 S_1(t-\tau_1)I_1(t-\tau_1) - (d+\delta_1)I_1\right] \\ &= \frac{\beta_1 S_1^* I_1^* e^{-d\tau_1}}{I_1^*}\left[\frac{S_1(t-\tau_1)I_1(t-\tau_1)}{S_1^* I_1^*} - \frac{I_1}{I_1^*}\right. \\ &\quad \left. - \frac{S_1(t-\tau_1)I_1(t-\tau_1)I_1^*}{S_1^* I_1^* I_1} + 1\right].\end{aligned} \tag{29}$$

$$\begin{aligned}\frac{dV_5}{dt} &= \int_0^{\tau_1} -\frac{d}{ds}\left(\frac{I_1(t-s)}{I_1^*} + 1 - \ln\frac{S_1(t-s)I_1(t-s)}{S_1^* I_1^*}\right)ds \\ &= \int_0^{\tau_1} -\frac{d}{ds}\left(\frac{I_1(t-s)}{I_1^*} + 1 - \ln\frac{S_1(t-s)I_1(t-s)}{S_1^* I_1^*}\right)ds \\ &= \frac{I_1}{I_1^*} - \frac{I_1(t-\tau_1)}{I_1^*} + \ln\frac{S_1(t-\tau_1)I_1(t-\tau_1)}{S_1^* I_1^*} - \ln\frac{S_1 I_1}{S_1^* I_1^*}.\end{aligned} \tag{30}$$

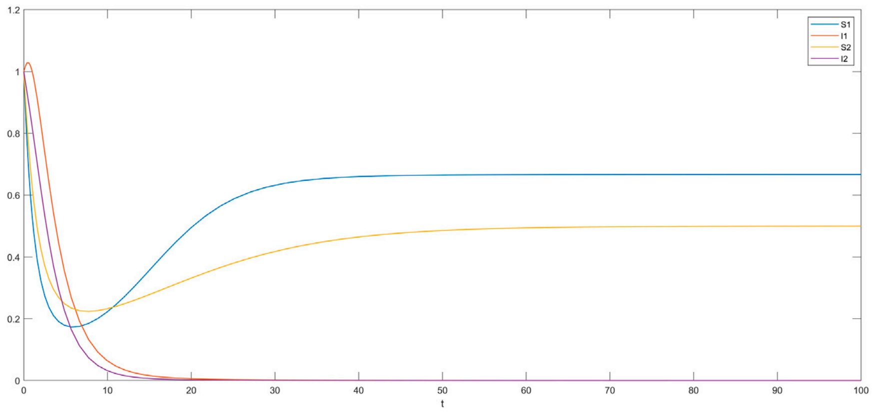

FIGURE 1
Stability of panic-free equilibrium when $R_0 < 1$.

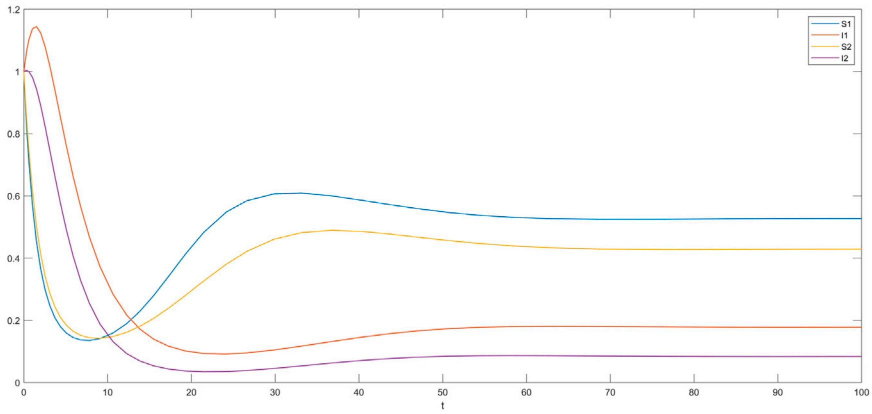

FIGURE 2
Stability of panic-permanent equilibrium when $R_0 > 1$.

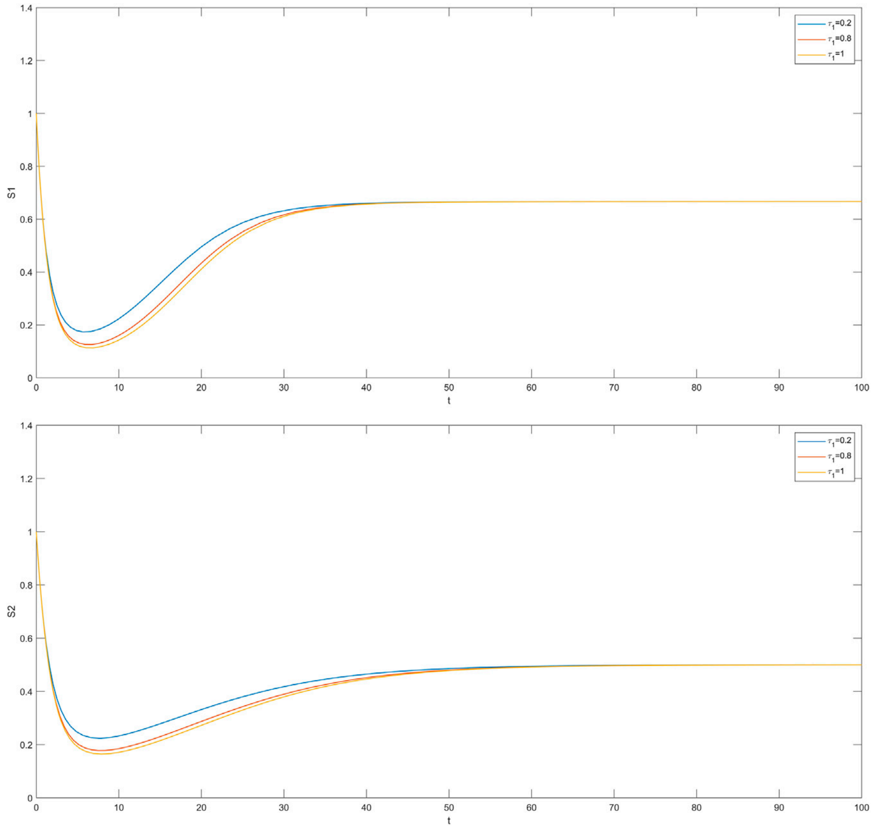

FIGURE 3
Trends of S_1 and S_2 with different time delays when $R_0 < 1$.

Thus, we can obtain

$$\begin{aligned}\frac{dV_2}{dt} &= -\frac{r_1}{K_1}(S_1 - S_1^*)^2 - \beta_1(S_1 - S_1^*)(I_1 - I_1^*)\\ &\quad -\left[\frac{S_1(t-\tau_1)I_1(t-\tau_1)}{S_1^* I_1^*} - 1 - \ln\frac{S_1(t-\tau_1)I_1(t-\tau_1)}{S_1^* I_1^*}\right]\\ &\quad -\frac{S_1(t-\tau_1)I_1(t-\tau_1)}{S_1^* I_1} - \frac{I_1(t-\tau_1)}{I_1^*} - \ln\frac{S_1 I_1}{S_1^* I_1^*}.\end{aligned} \tag{31}$$

Since $f(x) = x - 1 - \ln x \quad (x > 0)$, $\frac{dV_2}{dt} < 0$.

To prove that Model (5) is globally asymptotically stable, we consider the level-headed submodel.

$$\begin{aligned}\frac{dS_2}{dt} &= r_2 S_2\left(1 - \frac{S_2}{K_2}\right) - \beta_2 I_1^* S_2 - dS_2,\\ \frac{dI_2}{dt} &= e^{-d\tau_2}\beta_2 I_1^* S_2(t-\tau_2) - (d+\delta_2)I_2.\end{aligned} \tag{32}$$

The solution to the first equation is $S_2 = \frac{K_2(r_2 - \beta_2 I_1^* - d)}{r_2} + Ce^{-\frac{r_2}{K_2}t}$. Here, C is constant. Thus, $t \to \infty$ and $S_2 \to \frac{K_2(r_2 - \beta_2 I_1^* - d)}{r_2}$.

Considering the Lyapunov function,

$$\begin{aligned}V_6 &= I_2 + \int_0^{\tau_2} e^{-d\tau_2}\beta_2 S_2(t-s) I_1^* ds\\ &= -(d+\delta_2)I_2 - e^{-d\tau_2}\beta_2 S_2 I_1^* < 0.\end{aligned} \tag{33}$$

According to the LaSalle invariance principle, we further conclude that the panic-permanent equilibrium E^* is globally asymptotically stable for $R_0 > 1$.

4 Optimal control problem

4.1 Optimal control model

In this section, we denote the intensity of the government measures of the impatient group and the level-headed group, $u_1(t)$ and $\mu_2(t)$, as control variables to restrain the spread of panic during emergencies. Hence, we can obtain the optimal control model as follows:

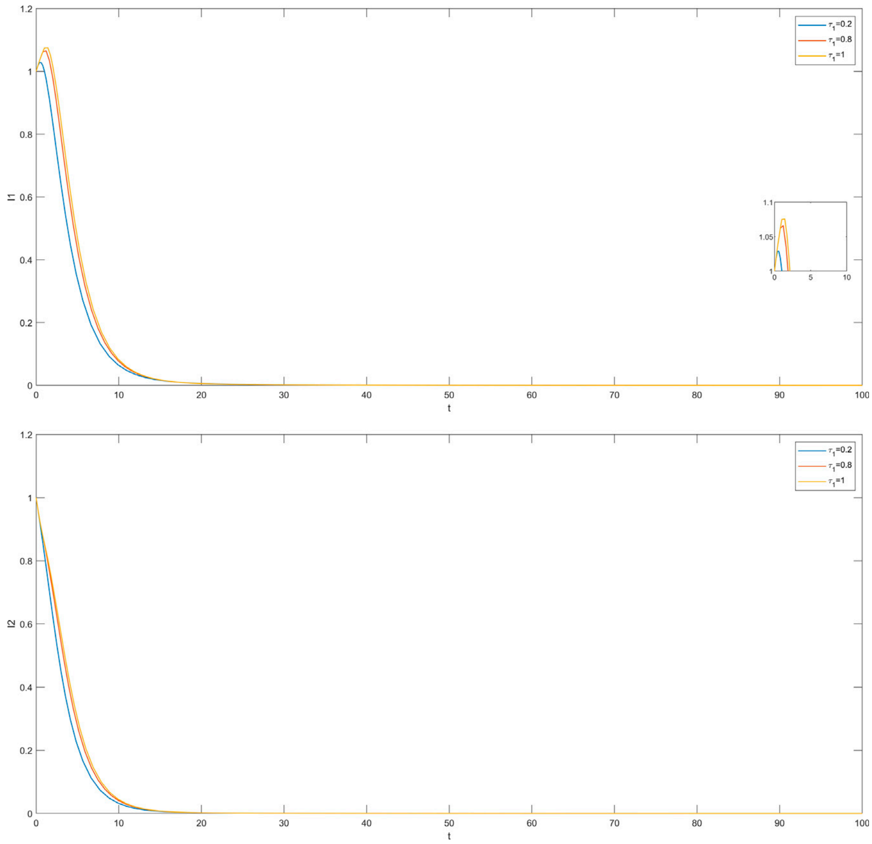

FIGURE 4
Trends of I_1 and I_2 with different time delays when $R_0 < 1$.

$$\begin{aligned}
\frac{dS_1}{dt} &= r_1 S_1\left(1-\frac{S_1}{K_1}\right)-\beta_1 I_1 S_1-(d+u_1(t))S_1,\\
\frac{dI_1}{dt} &= e^{-d\tau_1}\beta_1 S_1(t-\tau_1)I_1(t-\tau_1)-(d+\delta_1+u_1(t))I_1,\\
\frac{dS_2}{dt} &= r_2 S_2\left(1-\frac{S_2}{K_2}\right)-\beta_2 I_1 S_2-(d+\mu_2(t))S_2,\\
\frac{dI_2}{dt} &= e^{-d\tau_2}\beta_2 S_2(t-\tau_2)I_1(t-\tau_2)-(d+\delta_2+\mu_2(t))I_2,
\end{aligned} \tag{34}$$

with the initial conditions as follows:

$$\begin{cases} S_1(\theta)=\vartheta_1(\theta), I_1(\theta)=\vartheta_2(\theta), S_2(\theta)=\vartheta_3(\theta), I_2(\theta)=\vartheta_4(\theta),\\ \vartheta_i(\theta)\geq 0, \vartheta_i(0)>0, \theta\in[-\tau,0], (\vartheta_i\in C([-\tau,0],R_+^4), i=1,2,3,4. \end{cases} \tag{35}$$

We define the control set as

$$U=\{(u_2(t),u_2(t))\}|u_i(t) meansurable, u(t)\in[0,1], t\in[0,T]\}. \tag{36}$$

The goal of the control problem in this section is to take the intensity of the government measures that minimizes the number of infected individuals in the impatient group and the level-headed group and spread scale. Thus, for the control variables $u_i(t)$, $(i=1,2)$, the objective function can be defined by

$$J(u_1(t),u_2(t))=\frac{1}{2}\int_0^T[u_1(t)^2+u_2(t)^2]dt. \tag{37}$$

4.2 Existence of the optimal control model

Theorem 3.5. an optimal control pair $u^*(t)=(u_1^*,u_2^*)\in U$ exists so that

$$J(u_1^*,u_2^*)=\min_{(u_1,u_2)\in U} J(u_1,u_2).$$

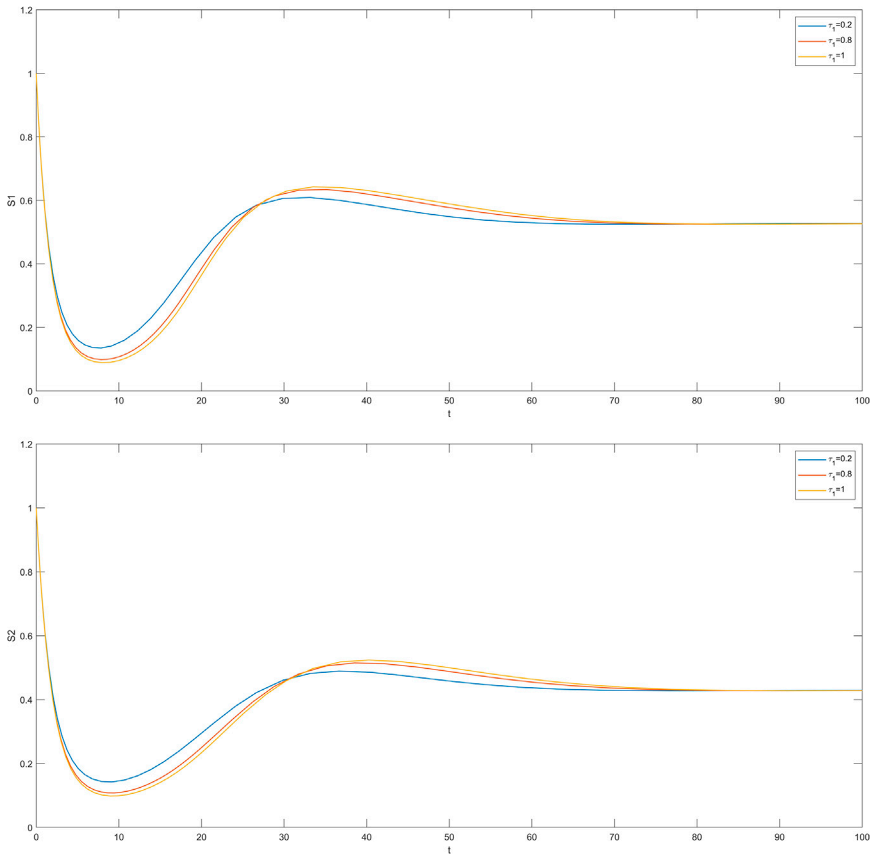

FIGURE 5
Trends of S_1 and S_2 with different time delays when $R_0 > 1$.

Proof. To prove the existence of an optimal solution for the model, we need to satisfy the following conditions:

(I) The state and control variables are non-negative.
(II) U is closed and bounded.
(III) The right-hand side of the state equation is continuous and bounded.
(IV) Since the control variables are quadratic functions, the objective function is convex.
(V) There exist constants $\omega_1 > 0, \omega_2 > 0, \kappa > 1$ such that

$$\frac{1}{2}\left(u_1^2 + u_2^2\right) \geq \omega_1\left(\sqrt[\kappa]{|u_1|^2 + |u_2|^2}\right) - \omega_2.$$

We use the results in [51]. We consider that the state and control variables are non-negative. Also, the control set U, by definition, is closed and bounded. Since $u_1(t)$ and $\mu_2(t)$ are linear, condition (III) is satisfied. Furthermore, the integrand (37) is convex due to the biquadratic and quadratic nature of control variables $u_1(t)$ and $\mu_2(t)$. Next, there exist constants $\omega_1 > 0, \omega_2 > 0, \kappa > 1$, and we have

$$\frac{1}{2}\left(u_1^2 + u_2^2\right) \geq \omega_1\left(\sqrt[\kappa]{|u_1|^2 + |u_2|^2}\right) - \omega_2.$$

We conclude that there exists optimal control.

Theorem 3.6. there exists an adjoint variable $\lambda_i(t), i = 1, 2, 3, 4$ that satisfies the following equations:

$$\begin{aligned}
\frac{d\lambda_1}{dt} &= -\Big\{\lambda_1(t)\Big[r_1 - \frac{2r_1S_1^*}{K_1} - \beta_1 I_1^* - (u_1(t) + d)\Big] \\
&\quad + \chi_{[0,T-\tau_1]}(t)\Big[\lambda_2(t+\tau_1)\beta_1 e^{-d\tau_1} I_1^*(t-\tau_1)\Big]\Big\}, \\
\frac{d\lambda_2}{dt} &= \lambda_1(t)\beta_1 S_1^* + \lambda_2(t)(d + \delta_1 + u_1(t)) + \lambda_3(t)\beta_2 S_2^* \\
&\quad - \Big\{\chi_{[0,T-\tau_1]}(t)\Big[\lambda_2(t+\tau_1)\beta_1 e^{-d\tau_1} S_1^*(t-\tau_1)\Big] \\
&\quad + \chi_{[0,T-\tau_2]}(t)\Big[\lambda_4(t+\tau_2)\beta_2 e^{-d\tau_2} S_2^*(t-\tau_2)\Big]\Big\}, \\
\frac{d\lambda_3}{dt} &= -\Big\{\lambda_3(t)\Big[r_2 - \frac{2r_2S_2^*}{K_2} \\
&\quad - \Big(d + u_2\big(t\big)\Big) - \beta_2 I_1^*\Big)\Big] + \chi_{[0,T-\tau_2]}(t)\Big[\lambda_4(t+\tau_2)\beta_2 e^{-d\tau_2} I_1^*(t-\tau_2)\Big]\Big\}, \\
\frac{d\lambda_4}{dt} &= \lambda_4(t)(d + \delta_2 + u_2),
\end{aligned} \tag{38}$$

10.3389/fphy.2022.1002512

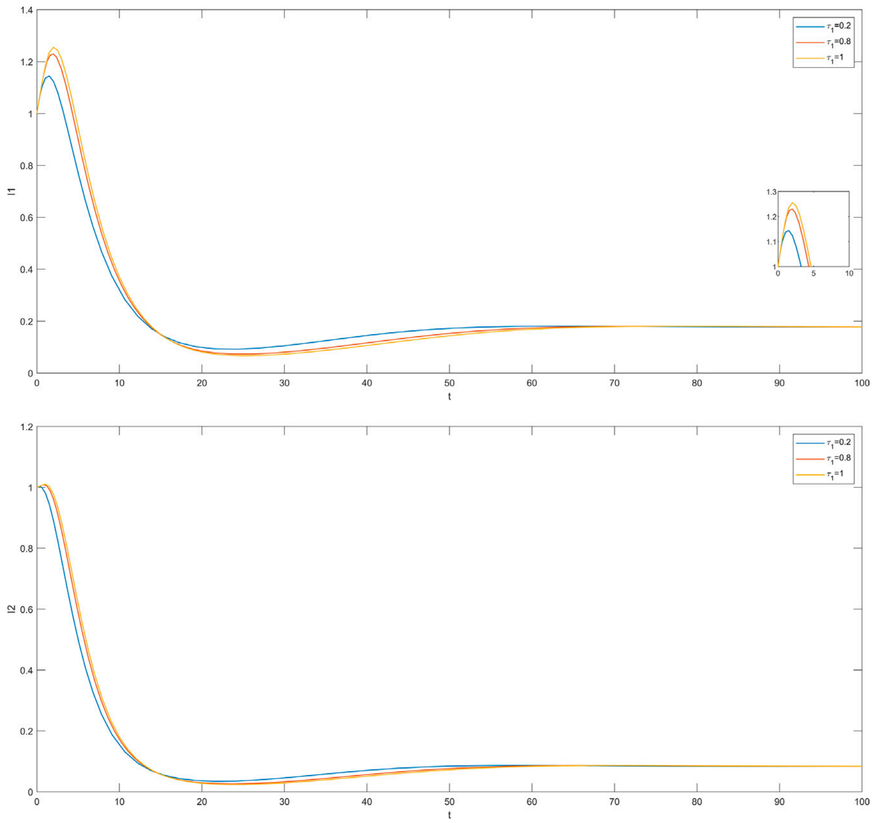

FIGURE 6
Trends of I_1 and I_2 with different time delays when $R_0 > 1$.

with boundary conditions: $\lambda_i(T) = 0$ $(i = 1, 2, 3, 4)$.

Furthermore, the optimal control variables are given as follows:

$$u_1^* = \max\{\min(\lambda_1(t)S_1^* + \lambda_2(t)I_1^*, \infty), 0\},$$

$$u_2^* = \max\{\min(\lambda_3(t)S_2^* + \lambda_4(t)I_2^*, \infty), 0\}.$$

Proof. We define the Hamiltonian as

$$\begin{aligned} H = &\frac{1}{2}(u_1^2 + u_2^2) + \lambda_1\left[r_1S_1\left(1 - \frac{S_1}{K_1}\right) - \beta_1 I_1 S_1 - (d + u_1)S_1\right] \\ &+\lambda_2\left[e^{-d\tau_1}\beta_1 S_1(t-\tau_1)I_1(t-\tau_1) - (d + \delta_1 + u_1)I_1\right] \\ &+\lambda_3\left[r_2S_2\left(1 - \frac{S_2}{K_2}\right) - \beta_2 I_1 S_2 - (d + \mu_2)S_2\right] \\ &+\lambda_4\left[e^{-d\tau_2}\beta_2 S_2(t-\tau_2)I_1(t-\tau_2) - (d + \delta_2 + \mu_2)I_2\right]. \end{aligned} \tag{39}$$

By differentiating the $S_1^*, I_1^*, S_2^*, I_2^*$ states in the Hamiltonian (39), we obtain the following adjoint equations:

$$\begin{aligned} \frac{d\lambda_1}{dt} &= -\left[\frac{\partial H}{\partial S_1}(t) + \chi_{[0,T-\tau_1]}(t)\frac{\partial H}{\partial S_1(t-\tau_1)}(t)\right], \\ \frac{d\lambda_2}{dt} &= -\left[\frac{\partial H}{\partial I_1}(t) + \chi_{[0,T-\tau_1]}(t)\frac{\partial H}{\partial I_1}(t) + \chi_{[0,T-\tau_2]}(t)\frac{\partial H}{\partial I_1(t-\tau_2)}(t)\right], \\ \frac{d\lambda_3}{dt} &= -\left[\frac{\partial H}{\partial S_2}(t) + \chi_{[0,T-\tau_2]}(t)\frac{\partial H}{\partial S_2(t-\tau_2)}(t)\right], \\ \frac{d\lambda_4}{dt} &= -\frac{\partial H}{\partial I_2}(t). \end{aligned} \tag{40}$$

According to the optimality condition,

$$\begin{cases} \dfrac{\partial H}{\partial u_1} = 0 \quad , \quad if\ u_1 = u_1^*, \\ \dfrac{\partial H}{\partial u_2} = 0 \quad , \quad if\ u_2 = u_2^*. \end{cases}$$

Thus, we can obtain $u_1^* = \lambda_1(t)S_1^* + \lambda_2(t)I_1^*, u_2^* = \lambda_3(t)S_2^* + \lambda_4(t)I_2^*$.

With the control set,

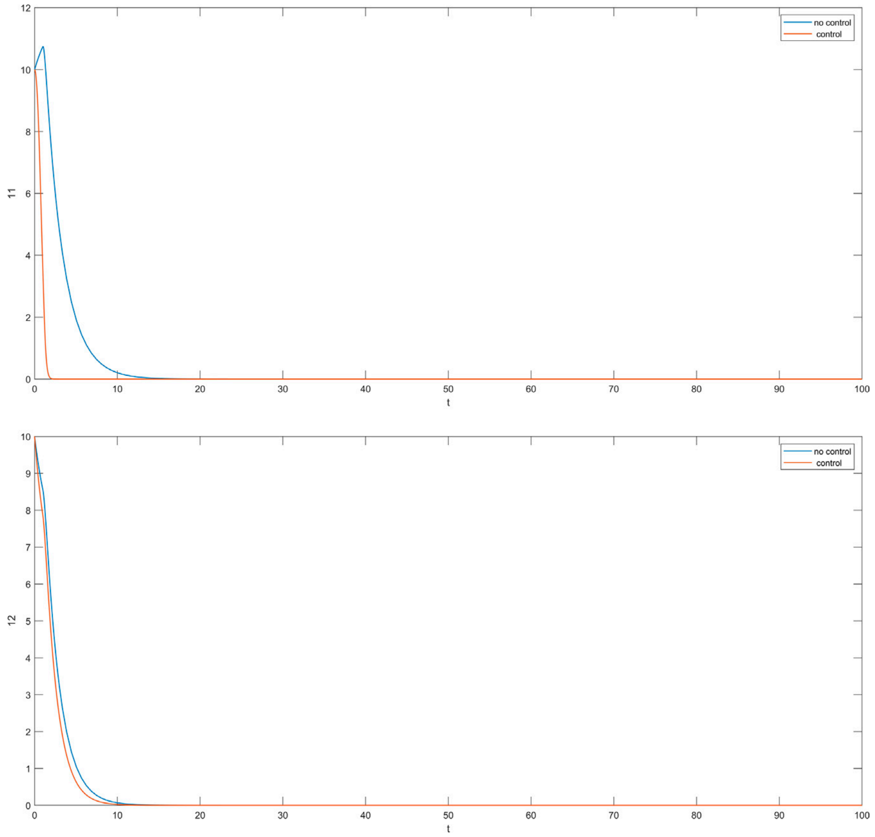

FIGURE 7
Comparison of trends of I_1 and I_2 with and without control.

$$u_1^* = \begin{cases} 0, & if\ \lambda_1(t)S_1^* + \lambda_2(t)I_1^* \le 0, \\ \lambda_1(t)S_1^* + \lambda_2(t)I_1^*, & if\ \ \lambda_1(t)S_1^* + \lambda_2(t)I_1^* > 0, \end{cases}$$

$$u_2^* = \begin{cases} 0, & if\ \lambda_3(t)S_2^* + \lambda_4(t)I_2^* \le 0, \\ \lambda_3(t)S_2^* + \lambda_4(t)I_2^*, & if\ \ \lambda_3(t)S_2^* + \lambda_4(t)I_2^* > 0., \end{cases}$$

The optimal control system at $(S_1^*, I_1^*, S_2^*, I_2^*, u_1^*, u_2^*, \lambda_1, \lambda_2, \lambda_3, \lambda_4)$ is

$$\begin{aligned} \frac{dS_1}{dt} &= r_1 S_1^*\left(1 - \frac{S_1^*}{K_1}\right) - \beta_1 I_1^* S_1^* - (d + u_1^*(t))S_1^*, \\ \frac{dI_1}{dt} &= e^{-d\tau_1}\beta_1 S_1^*(t-\tau_1)I_1^*(t-\tau_1) - (d + \delta_1 + u_1^*(t))I_1^*, \\ \frac{dS_2}{dt} &= r_2 S_2^*\left(1 - \frac{S_2^*}{K_2}\right) - \beta_2 I_1^* S_2^* - (d + u_2^*(t))S_2^*, \\ \frac{dI_2}{dt} &= e^{-d\tau_2}\beta_2 S_2^*(t-\tau_2)I_1^*(t-\tau_2) - (d + \delta_2 + u_2^*(t))I_2^*. \end{aligned} \tag{41}$$

With the corresponding adjoint system,

$$\begin{aligned} \frac{d\lambda_1}{dt} &= -\left\{\lambda_1(t)\left[r_1 - \frac{2r_1S_1^*}{K_1} - \beta_1 I_1^* - (u_1(t) + d)\right] +_{\chi[0,T-\tau_1]}(t) \left[\lambda_2(t+\tau_1)\beta_1 e^{-d\tau_1} I_1^*(t-\tau_1)\right]\right\}, \\ \frac{d\lambda_2}{dt} &= \lambda_1(t)\beta_1 S_1^* + \lambda_2(t)(d + \delta_1 + u_1(t)) + \lambda_3(t)\beta_2 S_2^* - \left\{_{\chi[0,T-\tau_1]}(t) \left[\lambda_2(t+\tau_1)\beta_1 e^{-d\tau_1} S_1^*(t-\tau_1)\right] +_{\chi[0,T-\tau 2]}(t) \left[\lambda_4(t+\tau_2)\beta_2 e^{-d\tau_2} S_2^*(t-\tau_2)\right]\right\}, \end{aligned} \tag{42}$$

$$\frac{d\lambda_3}{dt} = -\left\{\lambda_3(t)\left[r_2 - \frac{2r_2S_2^*}{K_2} - \left(d + u_2\left(t\right)\right) - \beta_2 I_1^*\right)\right] +_{\chi[0,T-\tau_2]}(t)\left[\lambda_4(t+\tau_2)\beta_2 e^{-d\tau_2} I_1^*(t-\tau_2)\right]\right\},$$

$$\frac{d\lambda_4}{dt} = \lambda_4(t)(d + \delta_2 + u_2).$$

5 Numerical simulation

5.1 Analysis of equilibrium

We set the values of the parameters as follows: $r_1 = 0.3$, $K_1 = 1$, $\beta_1 = 0.6$, $d = 0.1$, $\delta_1 = 0.35$, $r_2 = 0.2$, $K_2 = 1$, $\beta_2 = 0.4$, $\delta_2 = 0.45$, $\tau_1 = 0.2$, and $\tau_2 = 1$. The initial value is $(S_1(0), I_1(0), S_1(0), I_1(0)) = (1, 1, 1, 1)$. By calculation, we can obtain the panic-free equilibrium $E^0 = (0.67, 0, 0.5, 0)$, as shown in Figure 1.

The values of the parameters are as follows: $r_1 = 0.4$, $K_1 = 1$, $\beta_1 = 0.5$, $d = 0.1$, $\delta_1 = 0.15$, $r_2 = 0.3$, $K_2 = 1$, $\beta_2 = 0.4$, $\delta_2 = 0.25$, $\tau_1 = 0.2$, and $\tau_2 = 1$. As shown in Figure 2 we obtain the panic-permanent equilibrium $E^0 = (0.53, 0.18, 0.42, 0.08)$.

5.2 Analysis of the numerical simulation

In this section, we simulate the influence of different time delays on susceptible and infected individuals in the impatient group and the level-headed group. The time delay τ_1 takes different values ($\tau_1 = 0.2, 0.8, 1$), and $\tau_2 = 1$ is fixed.

The cases where $R_0 < 1$ are shown in Figures 3, 4. With the increase in time delay, the trend of susceptible individuals in both groups decreases first and then increases, with the minimum value decreasing. The peak of the infected individuals in the impatient group increases gradually, while the infected individuals in the level-headed group keep decreasing, indicating that different time delays have no effect on the infected individuals in the level-headed group. From Figure 4, the infected individuals in both groups tend toward zero when the panic in the group is extinct.

The cases where $R_0 > 1$ are shown in Figures 5, 6. The trend of susceptible individuals in both groups decreased sharply, while the trend of infected individuals increased abruptly in a short period of time. In the case with external environmental changes, the trend of susceptible individuals in both groups decreased sharply, while the trend of infected individuals increased abruptly in a short period of time. As time changes and the groups adapt to the environment, the infected individuals decrease, but they are always present. Eventually, the group reaches a steady state. From Figures 3–6, as the time delay increases, the peak of infected individuals increases. Therefore, the smaller the time delay is, the better the panic spreads. At the same time, the time delay has no effect on the stability of the panic-free equilibrium and the panic-permanent equilibrium. Thus, to effectively control panic spreading, the government must take measures that can increase the time delay and slow the spread of panic.

We consider that the intensity of the government measures can achieve the purpose of controlling the panic. The spread of panic is mainly dependent on the infected individuals. Therefore, Figure 7 indicates the comparison of trends of infected individuals in the two groups with and without control. On the one hand, a dramatic decrease in the trend of infected individuals with measures was derived. On the other hand, the time needed for the system to reach a steady state was reduced with measures. It can be seen that the control measures play an important role in the spread of panic and can effectively control the spread of panic.

6 Conclusion

In this study, the groups are divided into the impatient group and the level-headed group based on the psychological theory. Second, the susceptible individuals of the two groups are described by a single-species growth model. Third, a time-delayed panic-spreading model is established considering the influence of time delays for panic on the emotion transmission mechanism. The basic reproduction number of this model is calculated, and the conditions for the local and global asymptotic stability of the panic-free equilibrium and panic-permanent equilibrium are analyzed. To restrain the spread of emotions in emergencies, the government needs to take relevant measures, and the intensity of the measures taken is used to structure the optimal control model and minimize the control spread scale for emergencies. Finally, the related conclusions are illustrated by numerical simulations.

The aim of this study is to develop a model for simulating the spread process of panic. The results of the study are consistent with the trend of emotions in real situations. In the future, we will compare the results with those in other literature. Meanwhile, we simulate panic spreading in groups from a macroscopic perspective. Emotion spreading is a complex system from a microscopic perspective, considering the relationship between individuals and the external environment, and the rules of emotion spreading and interaction between individuals are also to be studied. Therefore, it is worth exploring emotion spreading in groups.

Data availability statement

The original contributions presented in the study are included in the article/Supplementary Material; further inquiries can be directed to the corresponding author.

Author contributions

Conceptualization: RL, HL, and QS. Data curation: RL. Formal analysis: RL. Funding acquisition: HL and QS. Investigation: RL. Methodology: RL. Project administration: HL and QS. Resources: HL and QS. Software: RL. Supervision: HL and QS. Validation: RL, HL, and QS. Visualization: RL. Writing—original draft: RL. Writing—review and editing: RL, HL, QS, and BL.

Funding

This research was funded by the Natural Science Foundation of China (71771112) and the Project of Liaoning Provincial Federation Social Science Circles of China (L20BGL047).

Conflict of interest

The authors declare that the research was conducted in the absence of any commercial or financial relationships that could be construed as a potential conflict of interest.

Publisher's note

All claims expressed in this article are solely those of the authors and do not necessarily represent those of their affiliated organizations, or those of the publisher, the editors, and the reviewers. Any product that may be evaluated in this article, or claim that may be made by its manufacturer, is not guaranteed or endorsed by the publisher.

References

1. Fu L, Song W, Lv W, Lo S. Simulation of emotional contagion using modified SIR model: A cellular automaton approach. *Physica A: Stat Mech its Appl* (2014) 405:380–91. doi:10.1016/j.physa.2014.03.043

2. Adam C, Gaudou B, Taillandier P. *Simulation of emotion dynamics in a group of agents in an evacuation situations*. Berlin, Germany: Springer-Verlag (2010). p. 604–19. doi:10.1007/978-3-642-25920-3_44

3. Zheng L, Peng X, Wang L, Sun D. Simulation of pedestrian evacuation considering emergency spread and pedestrian panic. *Physica A: Stat Mech its Appl* (2019) 522:167–81. doi:10.1016/j.physa.2019.01.128

4. Mao Y, Du X, Li Y, He W. An emotion based simulation framework for complex evacuation scenarios. *Graphical Models* (2019) 102:1–9. doi:10.1016/j.gmod.2019.01.001

5. Helbing D, Farkas I, Vicsek T. Simulating dynamical features of escape panic. *Nature* (2000) 407(6803):487–90. doi:10.1038/35035023

6. Li R, Li Y, Meng Z, Song Y, Jiang G. Rumor spreading model considering individual activity and refutation mechanism simultaneously. *IEEE Access* (2000) 8(99):63065–76. doi:10.1109/ACCESS.2020.2983249

7. Xia Y, Jiang H, Yu Z. Global dynamics of ILSR rumor spreading model with general nonlinear spreading rate in multi-lingual environment. *Chaos, Solitons & Fractals* (2022) 154:111698. doi:10.1016/j.chaos.2021.111698

8. Jing W, Li Y, Zhang X, Zhang J, Jin Z. A rumor spreading pairwise model on weighted networks. *Physica A: Stat Mech its Appl* (2022) 585:126451. doi:10.1016/j.physa.2021.126451

9. Zheng T, Nie LF, Teng Z, Luo Y. Modeling seasonal variation for mosquito-borne disease in the tropical monsoon environment. *Adv Differ Equ* (2020) 1: 469–16. doi:10.1186/s13662-020-02807-6

10. Sba B, Jg A, Fjc A, Sokolov IM, Lentz HH. Locally temperature - driven mathematical model of West Nile virus spread in Germany. *J Theor Biol* (2020) 488: 110117. doi:10.1016/j.jtbi.2019.110117

11. Tian Z, Zhang G, Hu C, Lu D, Liu H. Knowledge and emotion dual-driven method for crowd evacuation. *Knowledge-Based Syst* (2020) 208(11):106451. doi:10.1016/j.knosys.2020.106451

12. Yin F, Xia X, Pan Y, She Y, Feng X, Wu J. Sentiment mutation and negative emotion contagion dynamics in social media: A case study on the Chinese sina microblog. *Inf Sci* (2022) 594:118–35. doi:10.1016/j.ins.2022.02.029

13. Hu Y, Pan Q, Hou W, He M. Rumor spreading model considering the proportion of wisemen in the crowd. *Physica A: Stat Mech its Appl* (2018) 505: 1084–94. doi:10.1016/j.physa.2018.04.056

14. Jiang M, Gao Q, Zhuang J. Reciprocal spreading and debunking processes of online misinformation: A new rumor spreading–debunking model with a case study. *Physica A: Stat Mech its Appl* (2021) 565:125572. doi:10.1016/j.physa.2020.125572

15. Liu S, Ruan S, Zhang X. Nonlinear dynamics of avian influenza epidemic models. *Math Biosciences* (2017) 283:118–35. doi:10.1016/j.mbs.2016.11.014

16. Chen Y, Zhu S, He H. The influence of investor emotion on the stock market: Evidence from an infectious disease model. *Discrete Dyn Nat Soc* (2021) 9:1–12. doi:10.1155/2021/5520276

17. Zhao D, Li L, Peng H, Luo Q, Yang Y. Multiple routes transmitted epidemics on multiplex networks. *Phys Lett A* (2014) 378(10):770–6. doi:10.1016/j.physleta.2014.01.014

18. Zhao D, Wang L, Wang Z, Xiao G. Virus propagation and patch distribution in multiplex networks: Modeling, analysis, and optimal allocation. *IEEE Trans Inform Forensic Secur* (2019) 7(14):1755–67. doi:10.1109/TIFS.2018.2885254

19. Guo H, Yin Q, Xia C, Dehmer M. Impact of information diffusion on epidemic spreading in partially mapping two-layered time-varying networks. *Nonlinear Dyn* (2021) 105(4):3819–33. doi:10.1007/s11071-021-06784-7

20. Kang H, Fu C, Sun Z. Global exponential stability of periodic solutions for impulsive Cohen–Grossberg neural networks with delays. *Appl Math Model* (2015) 39(5–6):1526–35. doi:10.1016/j.apm.2014.09.015

21. Zhu L, Zhao H. Dynamical analysis and optimal control for a malware propagation model in an information network. *Neurocomputing* (2015) 149: 1370–86. doi:10.1016/j.neucom.2014.08.060

22. Huo L, Ma C. The interaction evolution model of mass incidents with delay in a social network. *Physica A: Stat Mech its Appl* (2017) 484:440–52. doi:10.1016/j.physa.2017.04.162

23. Li L, Fu J, Zhang Y, Chai T, Song L, Albertos P. Output regulation for networked switched systems with alternate event-triggered control under transmission delays and packet losses. *Automatica* (2021) 131:109716. doi:10.1016/j.automatica.2021.109716

24. Li J, Jin Z, Sun G. Periodic solutions of a spatiotemporal predator-prey system with additional food. *Chaos, Solitons & Fractals* (2016) 91:350–9. doi:10.1016/j.chaos.2016.06.010

25. Adak D, Bairagi N, Hakl R. Chaos in delay-induced Leslie–Gower prey–predator–parasite model and its control through prey harvesting – ScienceDirect. *Nonlinear Anal Real World Appl* (2020) 2020: 102998. doi:10.1016/j.nonrwa.2019.102998

26. Yu D, Wang G, Ding Q, Li T, Jia Y. Effects of bounded noise and time delay on signal transmission in excitable neural networks. *Chaos, Solitons & Fractals* (2022) 157:111929. doi:10.1016/j.chaos.2022.111929

27. Zheng T, Nie LF, Teng Z, Luo Y. Competitive exclusion in a multi-strain malaria transmission model with incubation period. *Chaos, Solitons & Fractals* (2020) 2020:109545. doi:10.1016/j.chaos.2019.109545

28. Wu W, Teng Z. Traveling waves in nonlocal dispersal SIR epidemic model with nonlinear incidence and distributed latent delay. *Adv Differ Equ* (2020) 1: 614–26. doi:10.1186/s13662-020-03073-2

29. Khan A, Ikram R, Din A, Humphries UW, Akgul A. Stochastic COVID-19 SEIQ epidemic model with time-delay. *Results Phys* (2021) 30:104775. doi:10.1016/j.rinp.2021.104775

30. Rihan FA, Alsakaji HJ. Dynamics of a stochastic delay differential model for COVID-19 infection with asymptomatic infected and interacting people: Case study in the UAE. *Results Phys* (2021) 28:104658. doi:10.1016/j.rinp.2021.104658

31. Xia C, Wang Z, Sanz J, Meloni S, Moreno Y. Effects of delayed recovery and nonuniform transmission on the spreading of diseases in complex networks. *Physica A: Stat Mech its Appl* (2013) 392(7):1577–85. doi:10.1016/j.physa.2012.11.043

32. Cheng Y, Huo L, Zhao L. Dynamical behaviors and control measures of rumor-spreading model in consideration of the infected media and time delay. *Inf Sci* (2021) 564(3):237–53. doi:10.1016/j.ins.2021.02.047

33. Zhang J, Wang X, Xie Y, Wang M. Research on multi-topic network public opinion propagation model with time delay in emergencies. *Physica A: Stat Mech its Appl* (2022) 600:127409. doi:10.1016/j.physa.2022.127409

34. Hu J, Zhu L. Turing pattern analysis of a reaction-diffusion rumor propagation system with time delay in both network and non-network environments. *Chaos, Solitons & Fractals* (2021) 153:111542. doi:10.1016/j.chaos.2021.111542

35. Bolzoni L, Bonacini E, Soresina C, Groppi M. Time-optimal control strategies in SIR epidemic models. *Math Biosci* (2017) 292:86–96. doi:10.1016/j.mbs.2017.07.011

36. Grandits P, Kovacevic RM, Veliov VM. Optimal control and the value of information for a stochastic epidemiological SIS-model. *J Math Anal Appl* (2019) 476:665–95. doi:10.1016/j.jmaa.2019.04.005

37. Dai F, Liu B. Optimal control problem for a general reaction-diffusion eco-epidemiological model with disease in prey. *Appl Math Model* (2020) 88:1–20. doi:10.1016/j.apm.2020.06.040

38. Kang T, Zhang Q, Rong L. A delayed avian influenza model with avian slaughter: Stability analysis and optimal control. *Physica A: Stat Mech its Appl* (2019) 529:121544. doi:10.1016/j.physa.2019.121544

39. Bashier EBM, Patidar KC. Optimal control of an epidemiological model with multiple time delays. *Appl Maths Comput* (2017) 292:47–56. doi:10.1016/j.amc.2016.07.009

40. Wu D, Bai Y, Yu C. A new computational approach for optimal control problems with multiple time-delay. *Automatica* (2019) 101:388–95. doi:10.1016/j.automatica.2018.12.036

41. Sun G, Zhang H, Chang L, Jin Z, Wang H, Ruan S. On the dynamics of a diffusive foot-and-mouth disease model with nonlocal infections. *SIAM J Appl Math* (2022) 82:1587–610. doi:10.1137/21M1412992

42. Kouidere A, Kada D, Balatif O, Rachik M, Naim M. Optimal control approach of a mathematical modeling with multiple delays of the negative impact of delays in applying preventive precautions against the spread of the COVID-19 pandemic with a case study of Brazil and cost-effectiveness. *Chaos, Solitons & Fractals* (2021) 2021:110438. doi:10.1016/j.chaos.2020.110438

43. Ma X, Luo X, Li L, Li Y, Sun GQ. The influence of mask use on the spread of COVID-19 during pandemic in New York City. *Results Phys* (2022) 34:105224. doi:10.1016/j.rinp.2022.105224

44. Yusra BR, Maheshsingh M, Abdel AHK, Oree V, Dauhoo MZ. Assessing the impact of contact tracing, quarantine and red zone on the dynamical evolution of the covid-19 pandemic using the cellular automata approach and the resulting mean field system: A case study in Mauritius. *Appl Math Model* (2022) 11:567–89. doi:10.1016/j.apm.2022.07.008

45. Jkkaa B, Eo C, Aa D, Moore SE, Sun GQ, Jin Z, et al. Optimal control and comprehensive cost-effectiveness analysis for COVID-19. *Results Phys* (2022) 33:105177. doi:10.1016/j.rinp.2022.105177

46. Mathide M, Raluca E, Antoine P, Saussereau B. A multi-strain epidemic model for COVID-19 with infected and asymptomatic cases: Application to French data. *J Theor Biol* (2022) 545:111117. doi:10.1016/j.jtbi.2022.111117

47. Cao M, Zhang G, Wang M, Lu D, Liu H. A method of emotion contagion for crowd evacuation. *Physica A: Stat Mech its Appl* (2017) 483:250–8. doi:10.1016/j.physa.2017.04.137

48. Crescenzo AD, Paraggio P, Román-Román P, Torres-Ruiz F. Applications of the multi-sigmoidal deterministic and stochastic logistic models for plant dynamics. *Appl Math Model* (2020) 92:884–904. doi:10.1016/j.apm.2020.11.046

49. Dreessche P, Watmough J. Reproduction numbers and sub-threshold endemic equilibria for compartmental models of disease transmission. *Math Biosci* (2002) 180(1-2):29–48. doi:10.1016/S0025-5564(02)00108-6

50. Heffernan JM, Smith RJ, Wahl LM. Perspectives on the basic reproductive ratio. *J R Soc Interf* (2005) 2(4):281–93. doi:10.1098/rsif.2005.0042

51. Lukes DL. *Differential equations: Classical to controlled*. New York: Academic Press (1982).